

# Comparative study of three-nucleon force models in $A = 3, 4$ systems

A. Kievsky,<sup>1</sup> M. Viviani,<sup>1</sup> L. Girlanda,<sup>2</sup> and L.E. Marcucci<sup>2</sup>

<sup>1</sup> *Istituto Nazionale di Fisica Nucleare,  
Largo Pontecorvo 3, 56127 Pisa, Italy*

<sup>2</sup> *Dipartimento di Fisica, Università di Pisa,  
Largo Pontecorvo 3, 56127 Pisa, Italy*

## Abstract

Using modern nucleon-nucleon interactions in the description of the  $A = 3, 4$  nuclei, it is not possible to reproduce both the three- and four-nucleon binding energies simultaneously. This is one manifestation of the necessity of including a three-nucleon force in the nuclear Hamiltonian. In this paper we will perform a comparative study of some, widely used, three-nucleon force models. We will analyze their capability to describe the aforementioned binding energies as well as the  $n - d$  doublet scattering length. A correct description of these quantities can be considered a stringent requirement for a nuclear Hamiltonian containing two- and three-nucleon interaction terms. As we will show, this requirement is not fulfilled by several of the models available in the literature. To satisfy it, we propose modifications in the parametrization of the three-nucleon forces and we study their effects on few selected  $N - d$  low energy scattering observables.

PACS numbers: 21.30.-x, 21.45.Ff, 27.10.+h

## I. INTRODUCTION

Realistic nucleon-nucleon (NN) potentials reproduce the experimental NN scattering data up to energies of 350 MeV with a  $\chi^2$  per datum close to 1. However, the use of these potentials in the description of the three- and four-nucleon bound and scattering states gives a  $\chi^2$  per datum much larger than 1 (see for example Ref. [1]). In order to improve that situation, different three-nucleon force (TNF) models have been introduced so far. Widely used in the literature are the Tucson-Melbourne (TM) and the Urbana IX (URIX) models [2, 3]. These models are based on the exchange mechanism of two pions between three nucleons. The TM model has been revisited within a chiral symmetry approach [4], and it has been demonstrated that the contact term present in it should be dropped. This new TM potential, known as TM', has been subsequently readjusted [5]. The final operatorial structure coincides with that one given in the TNF of Brazil already derived many years ago [6]. TNF models based on  $\pi\rho$  and  $\rho\rho$  meson exchange mechanisms have also been derived [7] and their effects have been studied in the triton binding energy [8]. More recently, TNFs have been derived [9] using a chiral effective field theory at next-to-next-to-leading order. A local version of these interactions (hereafter referred as N2LOL) can be found in Ref. [10]. At this particular order, the TNF has two unknown constants that have to be determined. More in general, all the models contain a certain number of parameters that fix the strength of the different terms that compose the interaction. It is a common practice to determine these parameters from the three- and four-nucleon binding energies. In the chiral effective field theory there is a consistent derivation of the two- and three-nucleon interactions and some of the low energy constants entering in the TNF are fixed already from the NN data. On the other hand, the parametrization of the TM' and URIX interactions have been determined in association with specific NN potentials. Therefore, their parametrizations could change when used with different NN potentials since different NN potentials predict different  $A = 3, 4$  binding energies.

The  $n - d$  doublet scattering length  $^2a_{nd}$  can give valuable information. In principle this quantity is correlated, to some extent, to the  $A = 3$  binding energy through the so-called Phillips line [11, 12]. However the presence of TNFs of the type studied here breaks this correlation. Therefore  $^2a_{nd}$  emerges as an independent observable that can be used to evaluate the capability of the interaction models to describe the low energy region. Due

to the lack of excited states in the  $A = 3$  system, the zero energy state is the first one above the ground state. In the case of  $n - d$  scattering at zero energy, the  $J = \frac{1}{2}^+$  state is orthogonal to the triton ground state and, for this reason, the wave function presents a node in the relative distance between the incident nucleon and the deuteron. The position of the node is related to the scattering length and it is also sensitive to the relation between the overall attraction and repulsion of the interaction. Several of the realistic NN potentials underestimate the triton binding energy. Adding a TNF, which in general can include an attractive as well as a repulsive component, with a strength fixed for example to reproduce the triton binding energy, the balance between the overall attraction and repulsion of the interaction changes with respect to that one produced by the NN potential alone. And, as we will show, this leads to different predictions of  $^2a_{nd}$  and the  $\alpha$ -particle binding energy  $B(^4\text{He})$ . An analysis of the parametrization of a chiral TNF, in order to describe the triton binding energy  $B(^3\text{H})$ ,  $B(^4\text{He})$  and  $^2a_{nd}$ , has been performed in Ref. [9]. A similar analysis has not been done for the local models URIX, TM' and N2LO since only the three- or four-body binding energy has been considered in the determination of their parametrization but not  $^2a_{nd}$ .

In Ref. [13] results for different combinations of NN interactions plus TNF models are given. We report the results for the quantities of interest in Table I. From the table, we can observe that the models are not able to describe simultaneously the  $A = 3, 4$  binding energies and  $^2a_{nd}$ . Triggered by this fact, in this paper we make a comparative study of the aforementioned TNF models. To this end we use the AV18 [14] as the reference NN interaction and the three-nucleon interaction models will be added to it. Parametrizations of the URIX and TM' models already exist in conjunction with the AV18 potential. Conversely the N2LO TNF has been constructed using the N3LO-Idaho potential from Ref. [15]. So, in a first step, we have adapted its parametrization in order to reproduce, in conjunction with the AV18 interaction,  $B(^3\text{H})$ . Successively, we study the sensitivity of different parametrizations in the description of  $B(^4\text{He})$  and  $^2a_{nd}$ . Selecting those parametrizations that predict these three quantities close to their experimental values, we study some polarization observables in  $p - d$  scattering at  $E_{lab} = 3$  MeV. As an interesting result, we have observed that the predictions of the different parametrizations fall in a narrow band that, in the case of the vector analyzing powers, has a different position for each model, indicating a sensitivity to the short range structure of the TNF.

All calculations have been done using the hyperspherical harmonics (HH) method as developed by some of the authors to describe bound and scattering states in  $A = 3, 4$  systems [16–19] in configuration space or in momentum space [20, 21] (for a recent review see Ref. [13]). The paper is organized as follows. In the next section we introduce the TNF models in configuration space defining their parametrizations. In Section III we make a sensitivity study of the parametrization for each model looking at  $B(^3\text{H})$ ,  $B(^4\text{He})$  and  $^2a_{nd}$ . In Section IV we study  $p - d$  polarization observables at  $E_{lab} = 3$  MeV for specific values of the parameters. The conclusions are given in the last section.

## II. THREE NUCLEON FORCE MODELS

In Ref. [13] the description of bound states and zero-energy states for  $A = 3, 4$  has been reviewed in the context of the HH method. In Table I we report results for the triton and  $^4\text{He}$  binding energies as well as for the doublet  $n - d$  scattering length  $^2a_{nd}$  using the AV18 and the N3LO-Idaho NN potentials and using the following combinations of two- and three-nucleon interactions: AV18+URIX, AV18+TM' and N3LO-Idaho+N2LOL. The results are compared to the experimental values also reported in the table. Worthy of notice is the recent very accurate datum for  $^2a_{nd}$  [22].

From the table we may observe that only the results obtained using an interaction model that includes a TNF are close to the corresponding experimental values. In the case of the AV18+TM', the strength of the TM' potential has been fixed to reproduce the  $^4\text{He}$  binding energy and, as can be seen from the table, the triton binding energy is underpredicted. Conversely, the strength of the URIX potential has been fixed to reproduce the triton binding energy, giving too much binding for  $^4\text{He}$ . The strength of the N2LOL potential has been fixed to reproduce simultaneously the triton and the  $^4\text{He}$  binding energies. In the three cases the predictions for the doublet scattering length are not in agreement with the experimental value, in particular for the AV18+URIX model.

Our intention is to study different parametrizations of the TNFs to obtain, as close as possible, a simultaneous description of the three quantities under observation. To this aim we give a brief description of the TM' (or Brazil), URIX and N2LOL models. Starting from

the following general TNF

$$W = \sum_{i < j < k} W(i, j, k) \quad , \quad (1)$$

a generic term can be put in the following form:

$$W(1, 2, 3) = aW_a(1, 2, 3) + bW_b(1, 2, 3) + dW_d(1, 2, 3) + c_D W_D(1, 2, 3) + c_E W_E(1, 2, 3) \quad . \quad (2)$$

Each term corresponds to a different mechanism and has a different operatorial structure. The first three terms arise from the exchange of two pions between three nucleons. The  $a$ -term comes from  $\pi N$   $S$ -wave scattering whereas the  $b$ -term and  $d$ -term, which are the most important, come from  $\pi N$   $P$ -wave scattering. The specific form of these three terms in configuration space is the following:

$$\begin{aligned} W_a(1, 2, 3) &= W_0(\boldsymbol{\tau}_1 \cdot \boldsymbol{\tau}_2)(\boldsymbol{\sigma}_1 \cdot \mathbf{r}_{31})(\boldsymbol{\sigma}_2 \cdot \mathbf{r}_{23})y(r_{31})y(r_{23}) \\ W_b(1, 2, 3) &= W_0(\boldsymbol{\tau}_1 \cdot \boldsymbol{\tau}_2)[(\boldsymbol{\sigma}_1 \cdot \boldsymbol{\sigma}_2)y(r_{31})y(r_{23}) \\ &\quad + (\boldsymbol{\sigma}_1 \cdot \mathbf{r}_{31})(\boldsymbol{\sigma}_2 \cdot \mathbf{r}_{23})(\mathbf{r}_{31} \cdot \mathbf{r}_{23})t(r_{31})t(r_{23}) \\ &\quad + (\boldsymbol{\sigma}_1 \cdot \mathbf{r}_{31})(\boldsymbol{\sigma}_2 \cdot \mathbf{r}_{31})t(r_{31})y(r_{23}) \\ &\quad + (\boldsymbol{\sigma}_1 \cdot \mathbf{r}_{23})(\boldsymbol{\sigma}_2 \cdot \mathbf{r}_{23})y(r_{31})t(r_{23})] \\ W_d(1, 2, 3) &= W_0(\boldsymbol{\tau}_3 \cdot \boldsymbol{\tau}_1 \times \boldsymbol{\tau}_2)[(\boldsymbol{\sigma}_3 \cdot \boldsymbol{\sigma}_2 \times \boldsymbol{\sigma}_1)y(r_{31})y(r_{23}) \\ &\quad + (\boldsymbol{\sigma}_1 \cdot \mathbf{r}_{31})(\boldsymbol{\sigma}_2 \cdot \mathbf{r}_{23})(\boldsymbol{\sigma}_3 \cdot \mathbf{r}_{31} \times \mathbf{r}_{23})t(r_{31})t(r_{23}) \\ &\quad + (\boldsymbol{\sigma}_1 \cdot \mathbf{r}_{31})(\boldsymbol{\sigma}_2 \cdot \mathbf{r}_{31} \times \boldsymbol{\sigma}_3)t(r_{31})y(r_{23}) \\ &\quad + (\boldsymbol{\sigma}_2 \cdot \mathbf{r}_{23})(\boldsymbol{\sigma}_3 \cdot \mathbf{r}_{23} \times \boldsymbol{\sigma}_1)y(r_{31})t(r_{23})] \quad , \end{aligned} \quad (3)$$

with  $W_0$  an overall strength. The  $b$ - and  $d$ -terms are present in the three models whereas the  $a$ -term is present in the TM' and N2LOL and not in URIX. In the first two models, the radial functions  $y(r)$  and  $t(r)$  are obtained from the following function

$$f_0(r) = \frac{12\pi}{m_\pi^3} \frac{1}{2\pi^2} \int_0^\infty dq q^2 \frac{j_0(qr)}{q^2 + m_\pi^2} F_\Lambda(q) \quad (4)$$

where  $m_\pi$  is the pion mass and

$$\begin{aligned} y(r) &= \frac{1}{r} f_0'(r) \\ t(r) &= \frac{1}{r} y'(r) \quad . \end{aligned} \quad (5)$$

The cutoff function  $F_\Lambda$  in the TM' or Brazil models is taken as  $F_\Lambda = [(\Lambda^2 - m_\pi^2)/(\Lambda^2 + q^2)]^2$ . In the N2LOL model it is taken as  $F_\Lambda = \exp(-q^4/\Lambda^4)$ . The momentum cutoff  $\Lambda$  is a

parameter of the model fixing the scale of the problem in momentum space. In the N2LO, it has been fixed to  $\Lambda = 500$  MeV, whereas in the TM' model the ratio  $\Lambda/m_\pi$  has been varied to describe the triton or  $^4\text{He}$  binding energy at fixed values of the constants  $a, b$  and  $d$ . In the literature the TM' potential has been used many times with typical values around  $\Lambda = 5 m_\pi$ .

In the URIX model the radial dependence of the  $b$ - and  $d$ -terms is given in terms of the functions

$$\begin{aligned} Y(r) &= e^{-x}/x \xi_Y \\ T(r) &= (1 + 3/x + 3/x^2)Y(r) \xi_T \end{aligned} \tag{6}$$

with  $x = m_\pi r$  and the cutoff functions are defined as  $\xi_Y = \xi_T = (1 - e^{-cr^2})$ , with  $c = 2.1 \text{ fm}^{-2}$ . This regularization has been used in the AV18 potential as well. Since the URIX model has been constructed in conjunction with the AV18 potential, the use of the same regularization was a choice of consistency. The relation between the functions  $Y(r), T(r)$  and those of the previous models is:

$$\begin{aligned} Y(r) &= y(r) + T(r) \\ T(r) &= \frac{r^2}{3}t(r) . \end{aligned} \tag{7}$$

With the definition given in Eq.(4), the asymptotic behavior of the functions  $f_0(r)$ ,  $y(r)$  and  $t(r)$  is:

$$\begin{aligned} f_0(r \rightarrow \infty) &\rightarrow \frac{3}{m_\pi^2} \frac{e^{-x}}{x} \\ y(r \rightarrow \infty) &\rightarrow -\frac{3e^{-x}}{x^2} \left(1 + \frac{1}{x}\right) \\ t(r \rightarrow \infty) &\rightarrow \frac{3}{r^2} \frac{e^{-x}}{x} \left(1 + \frac{3}{x} + \frac{3}{x^2}\right) . \end{aligned} \tag{8}$$

To be noticed that with the normalization chosen for  $f_0$ , the functions  $Y$  and  $T$  defined from  $y$  and  $t$  and those ones defined in the URIX model coincide at large separation distances. Conversely, they have a different short range behavior. Using the URIX  $Y(r), T(r)$  functions, the  $a$ -term has been included in the construction of the Illinois TNF model [23].

The last two terms in Eq.(2) correspond to a two-nucleon (2N) contact term with a pion emitted or absorbed ( $D$ -term) and to a three-nucleon (3N) contact interaction ( $E$ -term).

Their local form, in configuration space, derived in Ref. [10], is

$$\begin{aligned}
W_D(1, 2, 3) = & W_0^D(\boldsymbol{\tau}_1 \cdot \boldsymbol{\tau}_2) \{ (\boldsymbol{\sigma}_1 \cdot \boldsymbol{\sigma}_2) [y(r_{31})Z_0(r_{23}) + Z_0(r_{31})y(r_{23})] \\
& + (\boldsymbol{\sigma}_1 \cdot \mathbf{r}_{31})(\boldsymbol{\sigma}_2 \cdot \mathbf{r}_{31})t(r_{31})Z_0(r_{23}) \\
& + (\boldsymbol{\sigma}_1 \cdot \mathbf{r}_{23})(\boldsymbol{\sigma}_2 \cdot \mathbf{r}_{23})Z_0(r_{31})t(r_{23}) \} \\
W_E(1, 2, 3) = & W_0^E(\boldsymbol{\tau}_1 \cdot \boldsymbol{\tau}_2)Z_0(r_{31})Z_0(r_{23}) .
\end{aligned} \tag{9}$$

The constants  $W_0^D$  and  $W_0^E$  fix the strength of these terms. In the case of the URIX model the  $D$ -term is absent whereas the  $E$ -term is present without the isospin operatorial structure and it has been included as purely phenomenological, without justifying its form from a particular exchange mechanism. Its radial dependence has been taken as  $Z_0(r) = T^2(r)$ . In the N2LOL model, the function  $Z_0(r)$  is defined as

$$Z_0(r) = \frac{12\pi}{m_\pi^3} \frac{1}{2\pi^2} \int_0^\infty dq q^2 j_0(qr) F_\Lambda(q) \tag{10}$$

with the same cutoff function used before,  $F_\Lambda(q) = \exp(-q^4/\Lambda^4)$ . In the TM' model the  $D$ - and  $E$ -terms are absent.

Each model is now identified from the values assigned to the different constants. Following Refs. [5, 24], in the case of the TM' model, the values of the constants are  $a = -0.87 m_\pi^{-1}$ ,  $b = -2.58 m_\pi^{-3}$ , and  $d = -0.753 m_\pi^{-3}$ ; the strength  $W_0 = (gm_\pi/8\pi m_N)^2 m_\pi^4$  and the cutoff has been fixed to  $\Lambda = 4.756 m_\pi$  in order to describe correctly, associated to AV18,  $B(^4\text{He})$ . In Table I the calculations have been done using these values with  $g^2 = 197.7$ ,  $m_\pi = 139.6$  MeV,  $m_N/m_\pi = 6.726$  ( $m_N$  is the nucleon mass) as given in the original derivation of the TM potential.

In the URIX model the  $b$ - and  $d$ -terms are present, however with a fixed ratio based on the Fujita-Miyazawa diagram. The strength of these terms are:  $bW_0 = 4 A_{2\pi}^{PW}$  and  $d = b/4$ , with  $A_{2\pi}^{PW} = -0.0293$  MeV. The model includes a purely central repulsive term introduced to compensate the attraction of the previous term, which by itself would produce a large overbinding in infinite nuclear matter. It is defined as

$$W_E^{URIX}(1, 2, 3) = A_R T^2(r_{31}) T^2(r_{23}) \tag{11}$$

with  $A_R = 0.0048$  MeV.

In the N2LOL potential the constants of the  $a$ -,  $b$ -,  $d$ -,  $D$ - and  $E$ -terms are defined in the

following way:

$$\begin{aligned}
W_0 &= \frac{1}{12\pi^2} \left( \frac{m_\pi}{F_\pi} \right)^4 g_A^2 m_\pi^2 \\
W_0^D &= \frac{1}{12\pi^2} \left( \frac{m_\pi}{F_\pi} \right)^4 \left( \frac{m_\pi}{\Lambda_x} \right) \frac{g_A m_\pi}{8} \\
W_0^E &= \frac{1}{12\pi^2} \left( \frac{m_\pi}{F_\pi} \right)^4 \left( \frac{m_\pi}{\Lambda_x} \right) m_\pi
\end{aligned} \tag{12}$$

with  $a = c_1 m_\pi^2$ ,  $b = c_3/2$ ,  $d = c_4/4$ , and  $c_1 = -0.00081 \text{ MeV}^{-1}$ ,  $c_3 = -0.0032 \text{ MeV}^{-1}$ ,  $c_4 = -0.0054 \text{ MeV}^{-1}$  taken from Ref. [15]. The other two constants,  $c_D = 1.0$  and  $c_E = -0.029$ , have been determined in Ref. [10] from a fit to  $B(^3\text{H})$  and  $B(^4\text{He})$  using the N3LO-Idaho+N2LOL potential model. The numerical values of the constant entering in  $W_0$ ,  $W_0^D$  and  $W_0^E$  are  $m_\pi = 138 \text{ MeV}$ ,  $F_\pi = 92.4 \text{ MeV}$ ,  $g_A = 1.29$ , and the chiral symmetry breaking scale  $\Lambda_x = 700 \text{ MeV}$ .

In order to analyze the different short range structure of the TNF models, in Fig. 1 we compare the dimensionless functions  $Z_0(r)$ ,  $y(r)$  and  $T(r)$  for the three models under consideration. In the TM' model using the definition of Eq.(10) and using the corresponding cutoff function we can define:

$$Z_0^{TM}(r) = \frac{12\pi}{m_\pi^3} \frac{1}{2\pi^2} \int_0^\infty dq q^2 j_0(qr) \left( \frac{\Lambda^2 - m_\pi^2}{\Lambda^2 + q^2} \right)^2 = \frac{3}{2} \left( \frac{m_\pi}{\Lambda} \right) \left( \frac{\Lambda^2}{m_\pi^2} - 1 \right)^2 e^{-\Lambda r} . \tag{13}$$

This function is showed in the first panel of Fig. 1 as a dashed line. From the figure we can see that, in the case of the URIX model, the functions  $Z_0(r)$  and  $y(r)$  go to zero as  $r \rightarrow 0$ . This is not the case for the other two models and is a consequence of the regularization choice of the  $Y$  and  $T$  functions adopted in the URIX.

### III. PARAMETRIZATION STUDY OF THE THREE NUCLEON FORCES

In this section we study possible variations to the parametrization of the TNF models in order to describe the  $A = 3, 4$  binding energies and  $^2a_{nd}$ .

#### A. Tucson-Melbourne Force

We first study the TM' potential and we would like to see whether, using the AV18+TM' interaction, it is possible to reproduce simultaneously the triton binding energy and the



doublet  $n - d$  scattering length for some values of the parameters. The  $a$ -term gives a very small contribution to these quantities, therefore, in the following analysis we maintain it fixed at the value  $a = -0.87 \, m_\pi^{-1}$ . The analysis is shown in Fig. 2. In the left panel, the doublet  $n - d$  scattering length,  $^2a_{nd}$ , is given as a function of the parameter  $b$  (in units of its original value  $b_0 = -2.58 \, m_\pi^{-3}$ ) for different values of the cutoff  $\Lambda$  (in units of  $m_\pi$ ). The box in the figure includes those values of  $^2a_{nd}$  compatible with the experimental results. On each point of the curves, the value of the constant  $d$  has been varied to reproduce the triton binding energy. Its corresponding values (in units of its original value  $d_0 = -0.753 \, m_\pi^{-3}$ ) are given in the right panel as a function of  $b$ . Therefore, each point of the curves in both panels corresponds to a set of parameters that, in connection with the AV18 potential, reproduces the triton binding energy. The variations of the parameters given in Fig. 2 do not exhaust all the possibilities. The analysis has been done maintaining the attractive character of the  $b$ - and  $d$ -terms and, therefore, the lines in the left panels of the figure stop when one of the two parameters,  $b$  or  $d$  changes sign. We can observe that, with the AV18+TM' potential, there is a very small region in the parameters' phase space available for a simultaneous description of the triton binding energy and the doublet scattering length. This small region corresponds to a value of  $b$  around four times bigger than the original value  $b_0$  and  $d$  results to be almost zero. Moreover, the value of the cutoff  $\Lambda$  around  $3.8m_\pi$  is smaller than the values usually used with the TM' potential ( $\Lambda \approx 5m_\pi$ ).

To be noticed that, for negative values of the parameters  $a$ ,  $b$  and  $d$ , the TM' potential is attractive and it does not include explicitly a repulsive term. Added to a specific NN potential that underestimates the three-nucleon binding energy, it supplies the extra binding by fixing appropriately its strength. As mentioned in Sec. I, the scattering length is sensitive to the balance between the attractive part and the repulsive part of the complete interaction. Therefore, in the case of the TM' potential, it seems that introducing only attractive terms, fixed to reproduce the triton binding energy, it is difficult to reproduce correctly this balance.

As discussed before, the TM' potential is a modification of the original TM potential compatible with chiral symmetry. At next-to-next-to-leading order in the chiral effective field theory the  $D$ - and  $E$ -terms appear (see Ref. [9] and references therein) as given in Eq.(2). Here we introduce the following additional term to the TM' potential based on a

contact term of three nucleons

$$W_E^{TM}(1, 2, 3) = W_0^E Z_0^{TM}(r_{31})Z_0^{TM}(r_{23}) . \quad (14)$$

This term corresponds to the  $E$ -term in Eq. (2), except that, for the sake of simplicity, we have omitted the  $(\boldsymbol{\tau}_1 \cdot \boldsymbol{\tau}_2)$  operator. Its strength  $W_0^E$  is defined in Eq. (12) and the function  $Z_0^{TM}$ , defined in Eq. (13), is a positive function, therefore, for positive values of  $c_E$ , the new term is repulsive. We include it in the following analysis of the TM' potential. The results are shown in Fig. 3 for three values of  $\Lambda/m_\pi = 4, 4.8, 5.6$ . In the left panels the doublet  $n-d$  scattering length is given as a function of the parameter  $b$  (in units of  $b_0$ ) for different values of the strength  $c_E$  of the  $E$ -term. The box in the panels includes those values compatible with the experimental results. At each point of the curves, the value of the constant  $d$  has been varied to reproduce the triton binding energy. For selected values of the parameters inside the box, the predictions for the  ${}^4\text{He}$  binding energy,  $B({}^4\text{He})$ , are shown in the right panels.

Comparing the left panels in Figs. 2 and 3, the effect of the new term is clear. In Fig. 2 we have observed that using  $\Lambda \geq 4 m_\pi$ ,  ${}^2a_{nd}$  cannot be well reproduced. Conversely, in Fig. 3, the inclusion of the new term allows for a description of  ${}^2a_{nd}$  using different values of the cutoff. The values of the parameter  $b$  are closer to its original value as  $\Lambda$  increases. Opposite to this, the predictions of  $B({}^4\text{He})$  improves as  $\Lambda$  decreases. For example, considering the case  $\Lambda = 4 m_\pi$ ,  ${}^2a_{nd}$ ,  $B({}^3\text{H})$  and  $B({}^4\text{He})$  are well reproduced with  $b = 3.2b_0$ ,  $d = 6.2d_0$  and  $c_E = 1$ . With  $\Lambda = 4.8 m_\pi$  the set of parameters that gives the best description of the three quantities is  $b = 1.5b_0$ ,  $d = 4.5d_0$  and  $c_E = 1.6$ . And with  $\Lambda = 5.6 m_\pi$  they are  $b = 0.8b_0$ ,  $d = 3d_0$  and  $c_E = 2$ . Their different contributions to the triton binding energy are given in Table II, where we report the mean values of the kinetic energy and the NN potential energy as well as the mean values of the attractive part of the TNF,  $V_A(3N)$ , corresponding to the sum of the  $a$ ,  $b$  and  $d$ -terms, and the repulsive part,  $V_R(3N)$ , corresponding to the  $c_E$  term. The last two columns show  $B({}^4\text{He})$  and  ${}^2a_{nd}$ . For the sake of comparison, in the first row, the original values of the parameters have been considered ( $b = b_0$ ,  $d = d_0$  and  $c_E = 0$ ) with the value of the cutoff fixed to reproduce the triton binding energy ( $\Lambda = 4.8 m_\pi$ ). As we can observe, in this case  $B({}^4\text{He})$  is overestimated and  ${}^2a_{nd}$  is underestimated. When the  $E$ -term is considered, the description of  $B({}^4\text{He})$  improves and it seems that a low value of  $\Lambda$  is preferable. A further analysis of these parametrizations is given Sec. IV studying some

polarization observables at low energy.

## B. Urbana IX Force

In the following we analyze the URIX potential which has two parameters, called  $A_{2\pi}^{PW}$  and  $A_R$ . In this model the strength of the  $d$ -term is related to the strength of the  $b$ -term as  $d = b/4$ . The original values of the parameters have been fixed in Ref. [3] in conjunction with the AV18 NN potential and, from Table I, we observe that the model correctly describes the triton binding energy. However, it overestimates  $B(^4\text{He})$  and underestimates  $^2a_{nd}$ . In order to further analyze the origin of this behavior, we have varied the constants  $A_{2\pi}^{PW}$ ,  $A_R$  and the relative strength  $D_{2\pi}^{PW} = d/b$  of the  $b$ - and  $d$ -terms. The regularization parameter has been held fixed at its original value,  $c = 2.1 \text{ fm}^{-2}$ . For a given value of  $A_{2\pi}^{PW}$ , the values of  $A_R$  and  $D_{2\pi}^{PW}$  has been chosen to reproduce  $B(^3\text{H})$  and  $^2a_{nd}$ . The results are shown in Fig. 4. In panel (a),  $D_{2\pi}^{PW}$  is given as a function of  $A_{2\pi}^{PW}$  with  $A_R$  varying from 0.0176 MeV at  $A_{2\pi}^{PW} = -0.02 \text{ MeV}$  to 0.0210 MeV at  $A_{2\pi}^{PW} = -0.050 \text{ MeV}$ . These values of  $A_R$  are more than three times bigger than the original value of 0.0048 MeV. In panel (b) and (c) the results for  $^2a_{nd}$  and  $B(^4\text{He})$  are given respectively. The latter has not been included in the determination of the parameters, since  $D_{2\pi}^{PW}$  and  $A_R$  have been determined from the triton binding energy and  $^2a_{nd}$ , and is therefore a pure prediction. We observe a slightly overestimation of  $B(^4\text{He})$ , in particular for values of  $|A_{2\pi}^{PW}| > 0.04 \text{ MeV}$ , corresponding to values of  $D_{2\pi}^{PW} < 0.7$ .

With modifications of the parameters in the URIX force, we were able to describe reasonably well  $B(^3\text{H})$ ,  $^2a_{nd}$  and  $B(^4\text{He})$ . However, this has been achieved with a substantial increase of the repulsive term. In order to gain insight on the consequence of the new parametrizations in the quantities of interest, in Table III we report the mean values of the kinetic energy and the NN potential energy as well as the mean values of the attractive part of the TNF,  $V_A(3N)$ , corresponding to the sum of the  $b$  and  $d$ -terms, and the repulsive part,  $V_R(3N)$ , corresponding to the  $A_R$  term, for selected values of the parameters (indicated as points in Fig. 4). The last two columns show  $B(^4\text{He})$  and  $^2a_{nd}$ . For the sake of comparison, in the first row, the values obtained using the original AV18+URIX model are reported. From the table we observe that some of the values considered for  $D_{2\pi}^{PW}$  and  $A_R$  are quite far from the original ones. At the original value of  $A_{2\pi}^{PW}$ ,  $-0.0293 \text{ MeV}$ , the relative strength

now results to be  $D_{2\pi}^{PW} = 1$  and  $A_R = 0.0181$  MeV. As  $D_{2\pi}^{PW}$  diminishes,  $A_R$  tends to increase further with the consequence that the mean value  $V_R(3N)$  is more than three times larger than the value obtained using the original parameters (given in the first row). This is compensated by a lower mean value of the kinetic energy. A further analysis of the effects of the parametrizations given in Table III is performed in Sec. IV studying selected  $p - d$  polarization observables.

### C. N2LOL Force

The parameters  $c_1$ ,  $c_3$  and  $c_4$  of the N2LOL model have been taken from the the chiral N3LO NN force of Ref. [15], whereas the  $c_D$  and  $c_E$  parameters have been determined in Ref. [10], in conjunction with that NN force, by fitting  $B(^3\text{H})$  and  $B(^4\text{He})$ . Here we are going to use the N2LOL force in conjunction with the AV18 NN interaction, so we have to modify its parametrization since the amount of attraction to be gained is now different (see Table I). In the following we will call  $c_1^0$ ,  $c_3^0$  and  $c_4^0$  the values of these constants, given in Sec.II, determined in Ref. [15]. Among different possibilities, in Fig. 5 we show a new parametrization of the N2LOL interaction obtained by multiplying  $c_3^0$  and  $c_4^0$  by a factor  $c_0$  and maintaining  $c_1 = c_1^0$ . Then the parameters  $c_D$  and  $c_E$  have been determined from a fit to  $B(^3\text{H})$  and  $^2a_{nd}$ . They are shown on panel (a) as a function of  $c_0$ . Therefore, at a fixed value of  $c_0$ , with the set of parameters  $c_1 = c_1^0$ ,  $c_3 = c_0 c_3^0$ ,  $c_4 = c_0 c_4^0$  and the corresponding values of  $c_D$  and  $c_E$  extracted from the figure, the AV18+N2LOL interaction reproduces the  $B(^3\text{H})$  and  $^2a_{nd}$ . In panel (b) we show the stability obtained in the description of the doublet scattering length corresponding to the constant value chosen for the determination of the parameters,  $^2a_{nd} = 0.644$  fm. With the new set of parameters it is now possible to calculate  $B(^4\text{He})$ . This is shown in panel (c) and it is interesting to note that in all cases the value  $B(^4\text{He})=28.60$  MeV has been obtained. Modifying also the parameter  $c_1$  as  $c_1 = c_0 c_1^0$  slightly different values of  $c_D$  and  $c_E$  are obtained. Using these values to calculate  $B(^4\text{He})$ , again we obtain a constant value that is now  $= 28.55$  MeV. Similar analyses using slightly different values of the cutoff  $\Lambda$  around 500 MeV do not change these results.

In order to correctly describe  $B(^4\text{He})$ , after fixing  $B(^3\text{H})$  and  $^2a_{nd}$ , we now analyze a modification to the relative strength of the  $b$ - and  $d$ -terms which, in the previous analysis, was maintained at its original value of  $c_4^0/c_3^0 = 1.6875$ . To this end we perform a similar

study as has been done previously for the other TNF models. Fixing the constant  $c_1$  to its original value  $c_1^0$ ,  $c_3$ ,  $c_4$ ,  $c_D$  and  $c_E$  have been varied. The analysis is shown in Fig. 6 at the following four values of  $c_E = 0, 0.1, -0.03, -0.5$  and for the indicated values of  $c_D$  chosen to reproduce  ${}^2a_{nd}$  (left panels). The predictions for  $B({}^4\text{He})$  are given in the right panels for those values of the parameters that give a value of  ${}^2a_{nd}$  inside the box. At each point of the curves in the left panels and at the points in the right panels,  $c_4$  has been chosen to reproduce the triton binding energy. Due to the  $(\boldsymbol{\tau}_i \cdot \boldsymbol{\tau}_j)$  operator in the  $E$ -term of the N2LO potential, positive values of  $c_E$  makes this term attractive. Conversely, negative values of  $c_E$  makes this term repulsive. We have considered only one positive case,  $c_E = 0.1$ . Increasing further  $c_E$  we found it difficult to describe correctly  $B({}^4\text{He})$ . For negative values of  $c_E$  we have considered two cases,  $c_E = -0.03$ , which corresponds to the value given in Ref. [10], and  $c_E = -0.5$ . From the figure we observe an almost linear behavior of  ${}^2a_{nd}$ . There is a slight curvature for negative values of  $c_D$  in the upper three panels. The analysis of  $B({}^4\text{He})$  selects the values of  $c_D$ . We have found that the experimental value is well reproduced for the pairs  $(c_D = -0.5, c_E = 0.1)$ ,  $(c_D = -1, c_E = 0)$ ,  $(c_D = -1, c_E = -0.03)$ , and  $(c_D = -2, c_E = -0.5)$ .

In Table IV we report the mean values of the kinetic energy, the two-nucleon potential energy as well as the mean values of the attractive part of the TNF,  $V_A(3N)$ , and its repulsive part  $V_R(3N)$  for the selected values of the parameters that correspond to the best description of the three quantities under study. In the last two columns of the table,  $B({}^4\text{He})$  and  ${}^2a_{nd}$  are given. The contributions to  $V_A(3N)$  come from the  $a$ -,  $b$ -,  $d$  and  $D$ -terms, which are always attractive in the cases considered, and from the  $E$ -term in the first case. This term contributes to the repulsive part  $V_R(3N)$  in the last two cases. From the table we may observe that  $c_3$  and  $c_4$  results to be larger and smaller than their original values, respectively. This is a consequence of the simultaneous description of  $B({}^3\text{H})$  and  ${}^2a_{nd}$ . Furthermore, in the first three cases, the ratio  $c_4/c_3 \approx 0.46$ , is much smaller than the original ratio.

#### IV. ANALYSIS OF THE POLARIZATION OBSERVABLES

In the previous section we have studied different parametrizations of the TM', UR1X and N2LO TNF models in conjunction with the AV18 NN potential. The analysis has been done varying the parameters in order first to reproduce  $B({}^3\text{H})$  and then looking at

their dependence on  $^2a_{nd}$  and  $B(^4\text{He})$ . To improve the description of these quantities, some substantial modifications were necessary for the first two models. In the case of the TM' interaction we found opportune the inclusion of a repulsive term. In the analysis of the URIX interaction, the strength of the repulsive term resulted to be more than three times bigger than the original value and the relative strength of the  $b$ - and  $d$ -terms, originally fixed to  $1/4$ , has been also increased. In the case of the N2LOL interaction, some adjustment of the parameters was necessary, mainly due to the fact that the AV18 interaction is less attractive than the N3LO interaction, from which the N2LOL model has been originally parametrized. In this section we analyze the effects of the new parametrizations in observables that are not correlated to the binding energies or to  $^2a_{nd}$ . Some polarization observables in  $p-d$  scattering have this characteristic, in particular the vector and tensor analyzing powers. In Figs. 7, 8, 9 we show the differential cross section  $d\sigma/d\Omega$ , the vector polarization observables  $A_y$  and  $iT_{11}$  and the tensor polarization observables  $T_{20}$ ,  $T_{21}$  and  $T_{22}$  at  $E_{lab} = 3$  MeV for the different potential models compared to the results obtained using the original AV18+URIX interaction. In the figures, the cyan band collects the results obtained with the parameters given in the three last rows of Table II, from the second to the sixth row of Table III, and the three last rows of Table IV for each model respectively, whereas the solid line is the prediction of the original AV18+URIX model. As we can see, for each TNF model, the observables calculated using the different parametrizations, fixed from a simultaneous description of  $B(^3\text{H})$ ,  $^2a_{nd}$  and  $B(^4\text{He})$ , fall in bands which, in the case of the vector analyzing powers, have a different position for the three models. Since the models essentially differ in the definitions of the functions  $y(r)$ ,  $T(r)$  and  $Z_0(r)$ , this difference can be associated to the different short-range behavior of the TNF models. In Fig. 7 we observe that the AV18+TM' model, using the new parametrizations, does not give any improvement in the observables compared to the AV18+URIX predictions. Moreover  $iT_{11}$  and  $T_{21}$  are worse described. It should be observed that the AV18+TM' model, with the original parametrization, and the AV18+URIX give similar results for the observables (a small difference can be observed in the maximum of  $A_y$  being slightly higher for the former). Therefore the previous conclusions do not change if compared to the original AV18+TM' model. In Fig. 8 we observe that the new parametrizations of the AV18+URIX produce a much worse description of  $A_y$ ,  $iT_{11}$  and  $T_{21}$ . Since the vector analyzing powers are mainly described by the  $P$ -wave phase-shift and mixing parameters, we can conclude that they result to be poorly reproduced with the new

parametrizations. Conversely to what happened analyzing the previous models, in Fig. 9, we observe that the N2LO interaction produces an improvement in the description of  $A_y$  and  $iT_{11}$ . The well known discrepancy in these observables is now reduced and, in particular for  $A_y$ , the improvement is noticeable. In the case of the tensor analyzing powers, a slightly worse description of  $T_{21}$  between the two maxima is now observed. In general all TNFs of the type analyzed here have this effect in  $T_{21}$  indicating that a different mechanism, not present in the models, should be considered to improve the description of the minimum around  $75^\circ$ .

Finally we would like to comment on the fact that the vector analyzing powers,  $A_y$  and  $iT_{11}$ , calculated using different TNF models fall inside a band with a different position for each model. In Fig. 10 the three bands, extracted from Figs. 7,8,9, are shown explicitly and compared to original AV18+URIX model (solid line). We can clearly observe the different position of the bands with the best description obtained with the new parametrizations of the AV18+N2LO model and the worst description with those one of the AV18+URIX model. Since all the models inside the bands describe reasonably well  $B(^3\text{H})$ ,  $^2a_{nd}$  and  $B(^4\text{He})$ , we can conclude that the difference is a direct consequence of their different short range structure. A natural question is whether, with opportune modifications of their radial dependence, i.e. modifying the functions  $y(r)$ ,  $T(r)$  and  $Z_0(r)$ , it will be possible to improve further the description of these observables at  $E_{lab} = 3$  MeV and, eventually, obtain a  $\chi^2$  per datum close to one. A preliminary study in this direction has shown that a further improvement in the  $A_y$  and  $iT_{11}$  maxima is associated to a worse description of the  $T_{21}$  minimum. The particular structure of these observables is related to a bigger splitting in the  $^4P_J$  phase-shifts than the normal splitting produced by the two-nucleon forces, as discussed in Ref. [26]. In particular the  $^4P_{1/2}$  phase-shift has to be smaller and the mixing parameter  $\epsilon_{3/2-}$  has to be bigger. It is a general feature of the TNFs studied here that they tend to increase both,  $^4P_{1/2}$  and  $\epsilon_{3/2-}$ . To be more precise, in Table V we show the  $^4P_J$  phase-shifts and  $\epsilon_{3/2-}$  for the AV18 and AV18+URIX potential models, and for one selected set of the parameters of Tables II, III, IV corresponding to the new parametrizations of the AV18+TM', AV18+URIX and AV18+N2LO models (indicated in the table with an asterisk). In particular, parametrizations of the second row of Table II, fourth row of Table III and third row of Table IV have been used, respectively. In the last row of the table, the results from phase-shift analysis (PSA) of Ref. [26] are given. From the table we observe that the  $^4P_{1/2}$  phase-shift increases when the TNF models are added to the AV18 potential.

By itself this change will produce a much worse description of  $A_y$  and  $iT_{11}$ . However this is well compensated with the corresponding increase in  ${}^4P_{5/2}$  and  $\epsilon_{3/2-}$ . This is not the case with the minimum in  $T_{21}$ , for which a better description would be obtained lowering the AV18 value of  ${}^4P_{1/2}$ , as discussed in Ref. [26]. The other parametrizations given in Tables II, III, IV produce similar changes in the  ${}^4P_J$  parameters. From this observation we can conclude that the spin-isospin structure of the TNFs considered here is not sufficient to describe simultaneously  $B({}^3\text{H})$ ,  ${}^2a_{nd}$ ,  $B({}^4\text{He})$  and the vector and tensor analyzing powers at low energies.

## V. CONCLUSIONS

Stimulated by the fact that some of the widely used TNF models do not reproduce simultaneously the triton and the  ${}^4\text{He}$  binding energies and the  $n - d$  doublet scattering length, we have analyzed possible modifications to their parametrizations. To this end we have selected the AV18 as the reference two-nucleon force and, associated with it, we have varied the original parameters of the TM' and URIX models so as to improve the description of the three quantities mentioned. Furthermore, using the recent local form of a chiral TNF (we have called this model N2LOL), we have studied its parametrization associated to the AV18 interaction too. The analysis has proceeded in the following way. The three models under observation, TM', AV18 and N2LOL, have been written in configuration space as a sum of five terms, the  $a$ -,  $b$ -,  $d$ -,  $C$ - and  $E$ -terms. The first three, corresponding to a two-pion exchange process, are attractive. The last two, corresponding to contact terms, can be either attractive or repulsive. Not all the models include the five terms. In the TM' model only the  $a$ -,  $b$ - and  $d$ -terms are present and therefore, this model does not include explicitly a repulsive term. The URIX model includes the  $b$ -,  $d$ - and  $E$ -terms. This last term has been parametrized as repulsive in order to compensate the large overbinding produced by the first two terms in infinite nuclear matter. The N2LOL model includes the five terms.

The study has been started analyzing the AV18+TM' model. Maintaining fixed the strength of the  $a$ -term at its original value, we have varied the strengths of the  $b$ - and  $d$ -terms for several values of the cutoff parameter  $\Lambda$ . We have explored negative values of the strength parameters  $b$  and  $d$  in order to keep the attractive character of these terms. We have found it difficult to reproduce  ${}^2a_{nd}$  for reasonable values of the strength parameters.



This fact has motivated the subsequent step of introducing a repulsive term in the model. As a simple choice, we have introduced a purely central  $E$ -term and a corresponding  $Z_0(r)$  function, obtained using the monopole cutoff of the model. Including this term we were able to describe simultaneously  $B(^3\text{H})$  and  $^2a_{nd}$  for several values of the cutoff. A further selection among these values has been done from the calculation of  $B(^4\text{He})$ . We have observed that with  $\Lambda \leq 4.8 m_\pi$  it was possible to describe the three quantities reasonably well.

In the original AV18+URIX model the relative strength between the  $b$ - and  $d$ -terms was fixed. In the present analysis we have relaxed this condition increasing the number of parameter of the model from two to three, the strengths of the  $b$ -,  $d$ - and  $E$ -terms. Varying them, we have found it possible to describe the three quantities of interest for values of the parameters very different from their original ones. In particular, the strength of the repulsive term resulted more than three times larger than the original value. In the case of the AV18+N2LOL model, maintaining the strength of the  $a$ -term fixed to its original value, we have varied the parameters  $c_3$ ,  $c_4$ ,  $c_D$  and  $c_E$  in combinations that reproduce  $B(^3\text{H})$ . Then we have studied the dependence on  $^2a_{nd}$  and  $B(^4\text{He})$  of the different parametrizations. For fixed values of  $c_E$  we have calculated  $^2a_{nd}$  for different values of  $c_3$  and  $c_D$ . We have found that  $c_3 \geq 1.4c_3^0$  in order to describe simultaneously  $B(^3\text{H})$  and  $^2a_{nd}$ . The values of  $c_D$  has been selected from the analysis of  $B(^4\text{He})$ . Values of  $B(^4\text{He})$  compatible with the experimental value have been found in the four cases of  $c_E$  explored.

After making this sensitivity study we have selected, for each model, some combinations of the parameters that give the better description of  $B(^3\text{H})$ ,  $^2a_{nd}$  and  $B(^4\text{He})$  and we have calculated the differential cross section and the vector and tensor analyzing powers at  $E_{lab} = 3$  MeV. At this energy there are well established discrepancies between the predictions of the theoretical models and the experimental results. For example all potential models underestimate  $A_y$  (the so-called  $A_y$  puzzle) and  $iT_{11}$  and overestimate the central minimum in  $T_{21}$ . Some TNF models have been constructed *ad hoc* to improve the description of these observables at low energy [27]. However the models studied here, derived from the exchange of two pions and contact terms, are not able to solve these discrepancies. What we have observed in the present study is that after fixing the parameters of each model from the description of  $B(^3\text{H})$ ,  $^2a_{nd}$  and  $B(^4\text{He})$ , the description of the vector polarization observables lies in a narrow band, positioned differently for each model. The best description is given by the AV18+N2LOL model which, with respect to the original AV18+URIX model, reduces

appreciably the discrepancy in  $A_y$  and  $iT_{11}$ . However it gives a slightly worse description of the central minimum of  $T_{21}$ . The other two models do not improve the description of the observables, compared always to the original AV18+URIX. The modified TM' model gives similar results though  $iT_{11}$  is slightly worse whereas the results with the modified URIX model are definitely worse than the original model. The fact that for each model the  $A_y$  and  $iT_{11}$  predictions lie in a narrow band, indicates a connection between the short-range structure of the TNF and the polarization observables at low energies. From the analysis we can conclude that the smoother form of the  $y(r)$ ,  $T(r)$  and  $Z_0(r)$  functions of the N2LOL potential are preferable. To be noticed that the TM' and URIX models do not include a  $D$ -term. An extended analysis of these two models including it, will allow for a more stringent conclusion about the short-range structure of the TNF models. Preliminary studies in this direction are underway.

Finally, at the end of Sec. III, we have analyzed the  $^4P_J$  phase-shift parameters. The overall attractive character of the TNF makes larger the  $^4P_{1/2}$  and  $^4P_{5/2}$  parameters, compared to the ones obtained using a NN force alone, and has little effect on  $^4P_{5/2}$ . The mixing parameter  $\epsilon_{3/2-}$  is larger too. Depending on the relative increase of these parameters, the description of  $A_y$  and  $iT_{11}$  can improve, as in the case of the N2LOL model, but not the description of the central minimum of  $T_{21}$ . The spin-isospin structure of the TNF models studied here cannot lower the  $^4P_{1/2}$  phase-shift which seems to be necessary in order to improve the description of  $T_{21}$  in the minimum. A different mechanism has to be included in the structure of the TNF, as for example it has been proposed in Ref. [27]. Studies along this line are at present underway.

- 
- [1] A. Kievsky, M. Viviani, and S. Rosati, Phys. Rev. C **64**, 024002 (2001)
  - [2] S.A. Coon and W. Glöckle, Phys. Rev. C **23**, 1790 (1981)
  - [3] B.S. Pudliner, V. R. Pandharipande, J. Carlson, and R.B. Wiringa, Phys. Rev. Lett. **74**, 4396 (1995)
  - [4] J.L. Friar, D. Hüber, and U. van Kolck, Phys. Rev. C **59**, 53 (1999)
  - [5] S.A. Coon and H.K. Han, Few-Body Syst. **30**, 131 (2001)
  - [6] H.T. Coelho, T.K. Das, and M.R. Robilotta, Phys. Rev. C **28**, 1812 (1983); M.R. Robilotta

- and H.T. Coelho, Nucl. Phys. A **460**, 645 (1986)
- [7] S.A. Coon and M.T. Peña, Phys. Rev. C **48**, 2559 (1993)
  - [8] A. Stadler, J. Adam, Jr., H. Henning, and P.U. Sauer, Phys. Rev. C **51**, 2896 (1995)
  - [9] E. Epelbaum *et al.*, Phys. Rev. C **66**, 064001 (2002)
  - [10] P. Navratil, Few-Body Syst. **41**, 117 (2007)
  - [11] A.C. Phillips, Nucl. Phys. A **107**, 209 (1968)
  - [12] P.F. Bedaque, H.-W. Hammer, and U. van Kolck, Nucl. Phys. A **646**, 444 (1999)
  - [13] A. Kievsky, S. Rosati, M. Viviani, L.E. Marcucci, and L. Girlanda, J. Phys. G: Nucl. Part. Phys. **35**, 063101 (2008)
  - [14] R.B. Wiringa, V.G.J. Stoks, and R. Schiavilla, Phys. Rev. C **51** 38 (1995)
  - [15] D.R. Entem and R. Machleidt, Phys. Rev. C **68** 041001(R) (2003)
  - [16] A. Kievsky, M. Viviani, and S. Rosati, Nucl. Phys. A **577**, 511 (1994)
  - [17] A. Kievsky, Nucl. Phys. A **624**, 125 (1997)
  - [18] M. Viviani, A. Kievsky, and S. Rosati, Phys. Rev. C **71** 024006 (2005)
  - [19] R. Lazauskas *et al.*, Phys.Rev. C **71** 034004 (2005)
  - [20] M. Viviani, L.E. Marcucci, S. Rosati, A. Kievsky, and L. Girlanda, Few-Body Syst.**39**, 159 (2006)
  - [21] L.E. Marcucci, A. Kievsky, L. Girlanda, S. Rosati and M. Viviani, Phys. Rev. C **80**, 034003 (2009)
  - [22] K. Schoen *et al.*, Phys. Rev. C **67**, 044005 (2003)
  - [23] S.C. Pieper, V.R. Pandharipande, R.B. Wiringa, and J. Carlson, Phys. Rev. C **64**, 014001 (2001)
  - [24] A. Nogga, H. Kamada, W. Glöckle, and B.R. Barrett, Phys. Rev. C **65**, 054003 (2002)
  - [25] S. Shimizu *et al.*, Phys. Rev. C **52**, 1193 (1995)
  - [26] A. Kievsky, S. Rosati, W. Tornow, and M. Viviani, Nuc. Phys. A **607**, 402 (1996)
  - [27] A. Kievsky, Phys. Rev. C **60**, 034001 (1999)

TABLE I: The triton and  $^4\text{He}$  binding energies  $B$  (MeV), and doublet scattering length  $^2a_{nd}$  (fm) calculated using the AV18 and the N3LO-Idaho two-nucleon potentials, and the AV18+URIX, AV18+TM' and N3LO-Idaho+N2LOL two- and three-nucleon interactions. The experimental values are given in the last row.

Potential	$B(^3\text{H})$	$B(^4\text{He})$	$^2a_{nd}$
AV18	7.624	24.22	1.258
N3LO-Idaho	7.854	25.38	1.100
AV18+TM'	8.440	28.31	0.623
AV18+URIX	8.479	28.48	0.578
N3LO-Idaho+N2LOL	8.474	28.37	0.675
Exp.	8.482	28.30	$0.645 \pm 0.003 \pm 0.007$

TABLE II: Mean values of the triton kinetic energy and the two-nucleon potential energy  $V(2N)$ , and the attractive,  $V_A(3N)$ , and repulsive,  $V_R(3N)$ , contributions of the TNF to the triton binding energy using the AV18+TM' potential for the specified values of the parameters and with  $a = -0.87 m_\pi^{-1}$ . In the last two columns  $B(^4\text{He})$  and  $^2a_{nd}$  are given respectively. The experimental values are given in the last row.

$b$	$d$	$c_E$	$\Lambda$	$T$	$V(2N)$	$V_A(3N)$	$V_R(3N)$	$B(^4\text{He})$	$^2a_{nd}$
$[m_\pi^{-3}]$	$[m_\pi^{-3}]$		$[m_\pi]$	[MeV]	[MeV]	[MeV]	[MeV]	[MeV]	[fm]
-2.580	-0.753	0.0	4.8	50.708	-58.144	-1.039	0.0	28.52	0.596
-8.256	-4.690	1.0	4.0	50.317	-57.366	-2.206	0.781	28.30	0.644
-3.870	-3.375	1.6	4.8	50.699	-57.641	-2.748	1.215	28.38	0.644
-2.064	-2.279	2.0	5.6	50.998	-57.940	-2.814	1.291	28.44	0.640
Exp.								28.30	$0.645 \pm 0.003 \pm 0.007$

TABLE III: Mean values of the triton kinetic energy, the two-nucleon potential energy  $V(2N)$ , and the attractive,  $V_A(3N)$ , and repulsive,  $V_R(3N)$ , contributions of the TNF to the triton binding energy using the AV18+URIX potential for the specified values of the parameters. In the last two columns  $B(^4\text{He})$  and  $^2a_{nd}$  are given respectively. The experimental values are given in the last row.

$A_{2\pi}^{PW}$	$D_{2\pi}^{PW}$	$A_R$	$T$	$V(2N)$	$V_A(3N)$	$V_R(3N)$	$B(^4\text{He})$	$^2a_{nd}$
[MeV]		[MeV]	[MeV]	[MeV]	[MeV]	[MeV]	[MeV]	[fm]
-0.0293	0.25	0.0048	51.259	-58.606	-1.126	1.000	28.48	0.578
-0.0200	1.625	0.0176	47.472	-57.976	-0.923	2.950	28.33	0.644
-0.0250	1.25	0.0182	47.628	-57.967	-1.162	3.024	28.34	0.644
-0.0293	1.00	0.0181	47.876	-58.000	-1.369	3.015	28.33	0.643
-0.0350	0.8125	0.0191	47.998	-57.975	-1.649	3.147	28.33	0.645
-0.0400	0.6875	0.0198	48.133	-57.964	-1.897	3.249	28.38	0.645
-0.0450	0.5625	0.0198	48.414	-57.995	-2.148	3.248	28.38	0.643
-0.0500	0.50	0.0210	48.471	-57.952	-2.401	3.401	28.44	0.645
Exp.							28.30	$0.645 \pm 0.003 \pm 0.007$

TABLE IV: Mean values of the triton kinetic energy, the two-nucleon potential energy  $V(2N)$ , and the attractive,  $V_A(3N)$ , and repulsive,  $V_R(3N)$ , TNF contributions to the triton potential energy using the AV18+N2LOL potential for the specified values of the parameters and with  $c_1 = -0.00081 \text{ MeV}^{-1}$ . In the last two columns  $B(^4\text{He})$  and  $^2a_{nd}$  are given. The experimental values are given in the last row.

$c_3$	$c_4$	$c_D$	$c_E$	$T$	$V(2N)$	$V_A(3N)$	$V_R(3N)$	$B(^4\text{He})$	$^2a_{nd}$
$[c_3^0]$	$[c_4^0]$			[MeV]	[MeV]	[MeV]	[MeV]	[MeV]	[fm]
1.4	0.3636	-0.5	0.1	49.834	-57.278	-1.029	0.0	28.31	0.641
1.4	0.3786	-1	0.0	49.950	-57.401	-1.022	0.0	28.30	0.636
1.5	0.3735	-1	-0.03	49.839	-57.274	-1.076	0.036	28.29	0.644
1.7	0.9000	-2	-0.50	50.166	-57.181	-2.119	0.657	28.32	0.645
Exp.								28.30	$0.645 \pm 0.003 \pm 0.007$

TABLE V: The  ${}^4P_J$  phase-shifts and the  $\epsilon_{3/2-}$  mixing parameter at  $E_{lab} = 3$  MeV for the potential models indicated. For the sake of comparison, the results of the PSA from Ref. [26] are given in the last row.

	${}^4P_{1/2}$	${}^4P_{3/2}$	${}^4P_{5/2}$	$\epsilon_{3/2-}$
AV18	22.03	24.24	24.08	-2.247
AV18+URIX	22.31	24.30	24.27	-2.314
AV18+TM'*	22.79	24.45	24.53	-2.453
AV18+URIX*	22.75	24.41	24.35	-2.375
AV18+N2LOL*	22.55	24.25	24.48	-2.394
PSA	$21.77 \pm 0.01$	$24.30 \pm 0.01$	$24.26 \pm 0.01$	$-2.46 \pm 0.01$

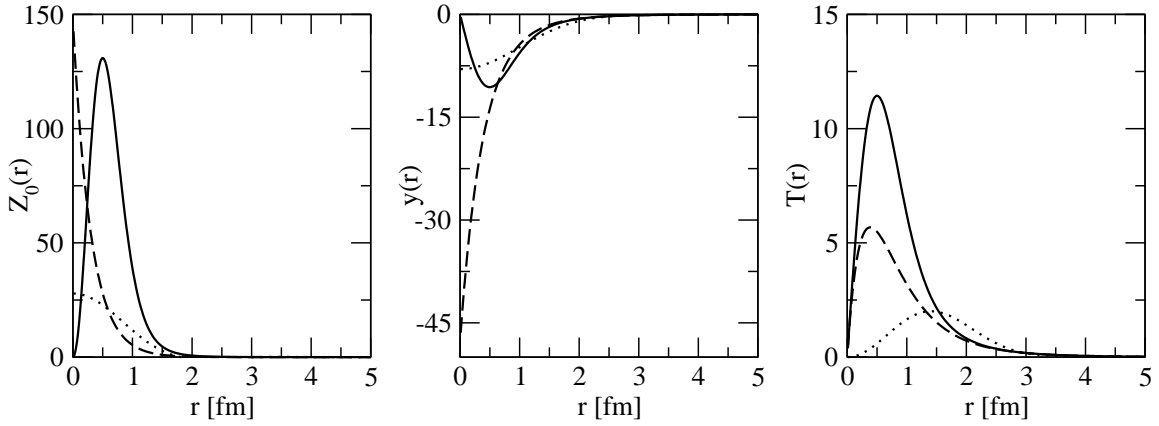


FIG. 1: The  $Z_0(r)$ ,  $y(r)$  and  $T(r)$  functions as functions of the interparticle distance  $r$  for the URIX (solid line), TM' (dashed line) and N2LOL (dotted line) models.

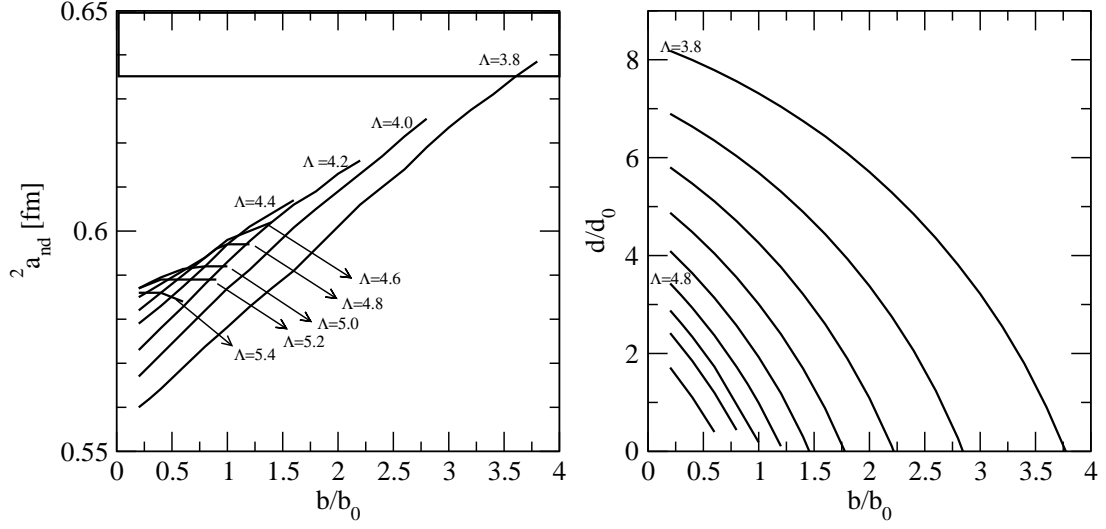


FIG. 2: The doublet scattering length  $^2a_{nd}$  as a function of the parameter  $b$  (in units of the original parameter  $b_0 = -2.58 \text{ m}_\pi^{-3}$ ) of the TM' potential for different values of the cutoff and the corresponding values of the parameter  $d$  (in units of the original parameter  $d_0 = -0.753 \text{ m}_\pi^{-3}$ ), as a function of the parameter  $b$ , used to reproduce the triton binding energy.

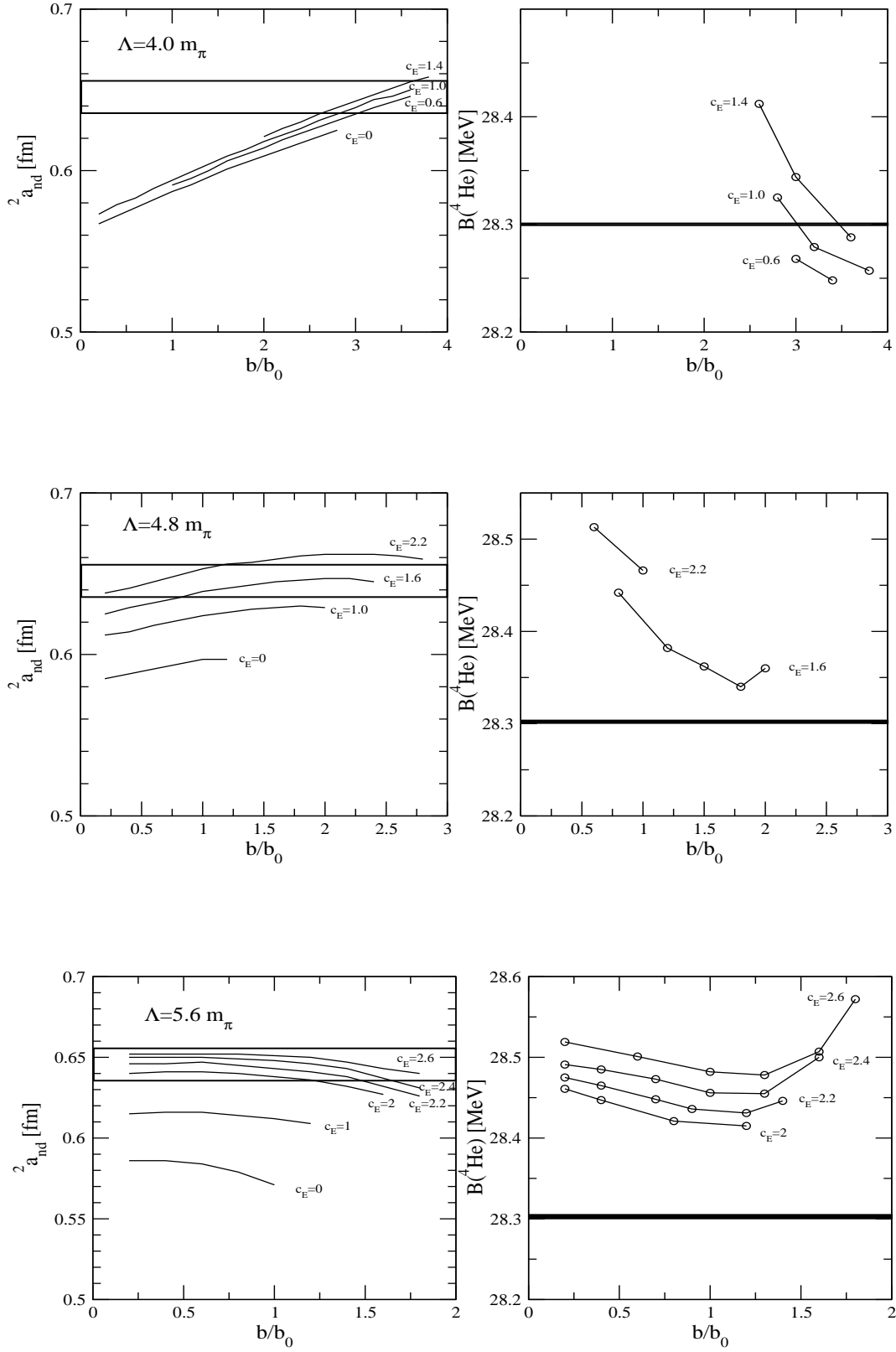


FIG. 3: The doublet scattering length  $a_{nd}$  as a function of the parameter  $b$  (in units of  $b_0 = -2.58 m_\pi^{-3}$ ) of the TM' potential including the  $W_E^{TM}$ -term, for different values of the strength  $c_E$  and for three selected values of  $\Lambda$ . The corresponding values of  $B(^4\text{He})$ , for specific values of  $a_{nd}$  inside the box, are shown in the right panels (circles).



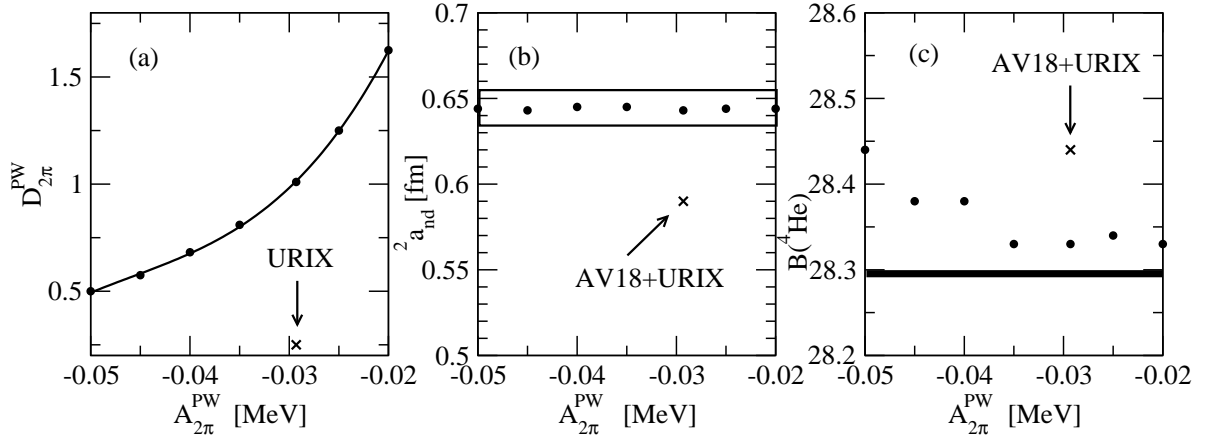


FIG. 4: (a) The relative strength  $D_{2\pi}^{PW}$ , (b)  $^2a_{nd}$  and (c)  $B(^4\text{He})$  as functions of  $A_{2\pi}^{PW}$ , for the AV18+URIX model.

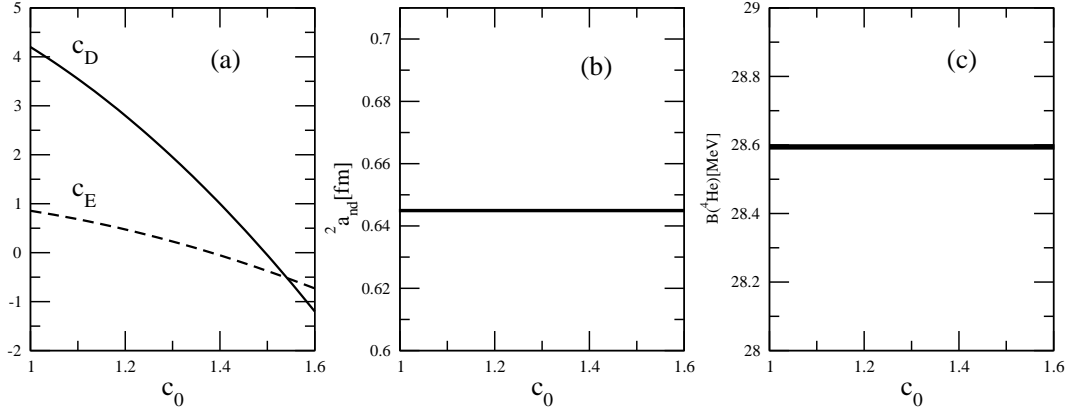


FIG. 5: (a) The  $c_D$  and  $c_E$  parameters, (b)  $^2a_{nd}$  and (c)  $B(^4\text{He})$ , as functions of  $c_0$ , for the AV18+N2LOL model.

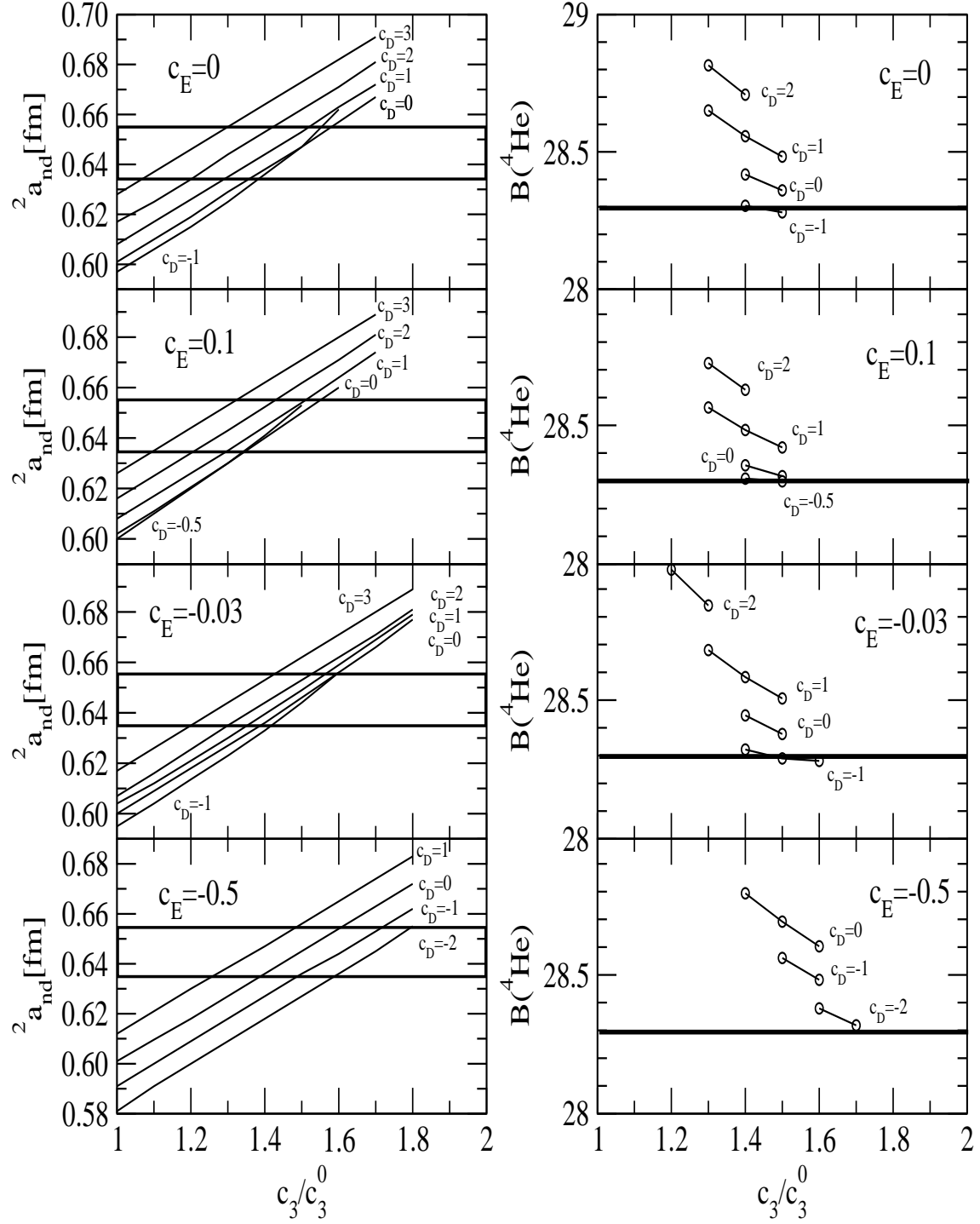


FIG. 6: The doublet scattering length  $^2a_{nd}$  as a function of the parameter  $c_3$  (in units of  $c_3^0 = -0.0032 \text{ MeV}^{-1}$ ) of the N2LOL potential, for different values of the strength  $c_D$ , at four selected values of  $c_E$ . The corresponding values of  $B(^4\text{He})$ , for specific values of  $a_{nd}$  inside the box, are shown in the right panels (circles).

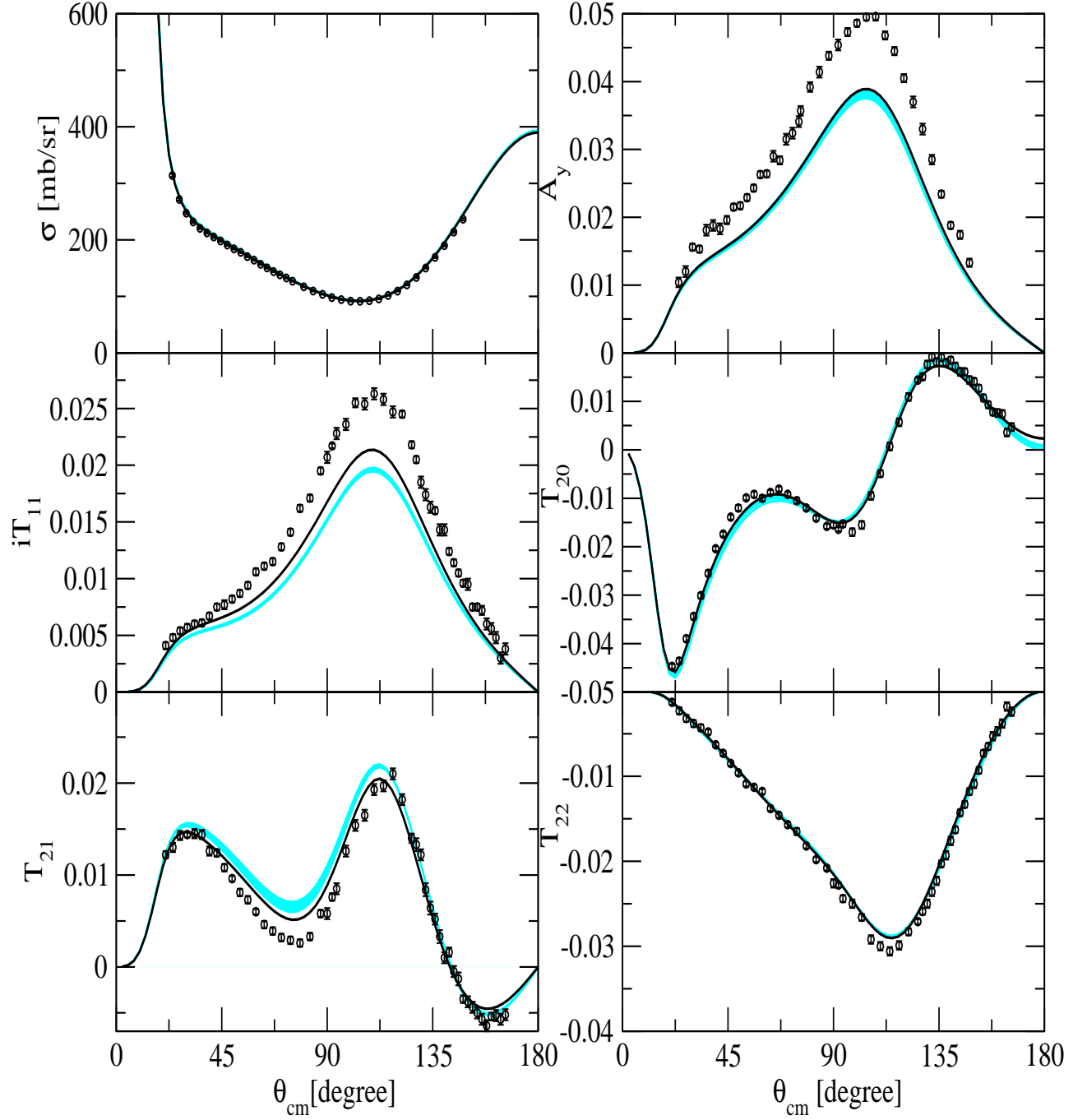


FIG. 7: (Color on line) Differential cross section and vector and tensor polarization observables at  $E_{\text{lab}} = 3$  MeV using the AV18+TM' model with the parameters given in the last three rows of Table II (cyan band). The predictions of the AV18+URIX model (solid line) and the experimental points from Ref. [25] are also shown.

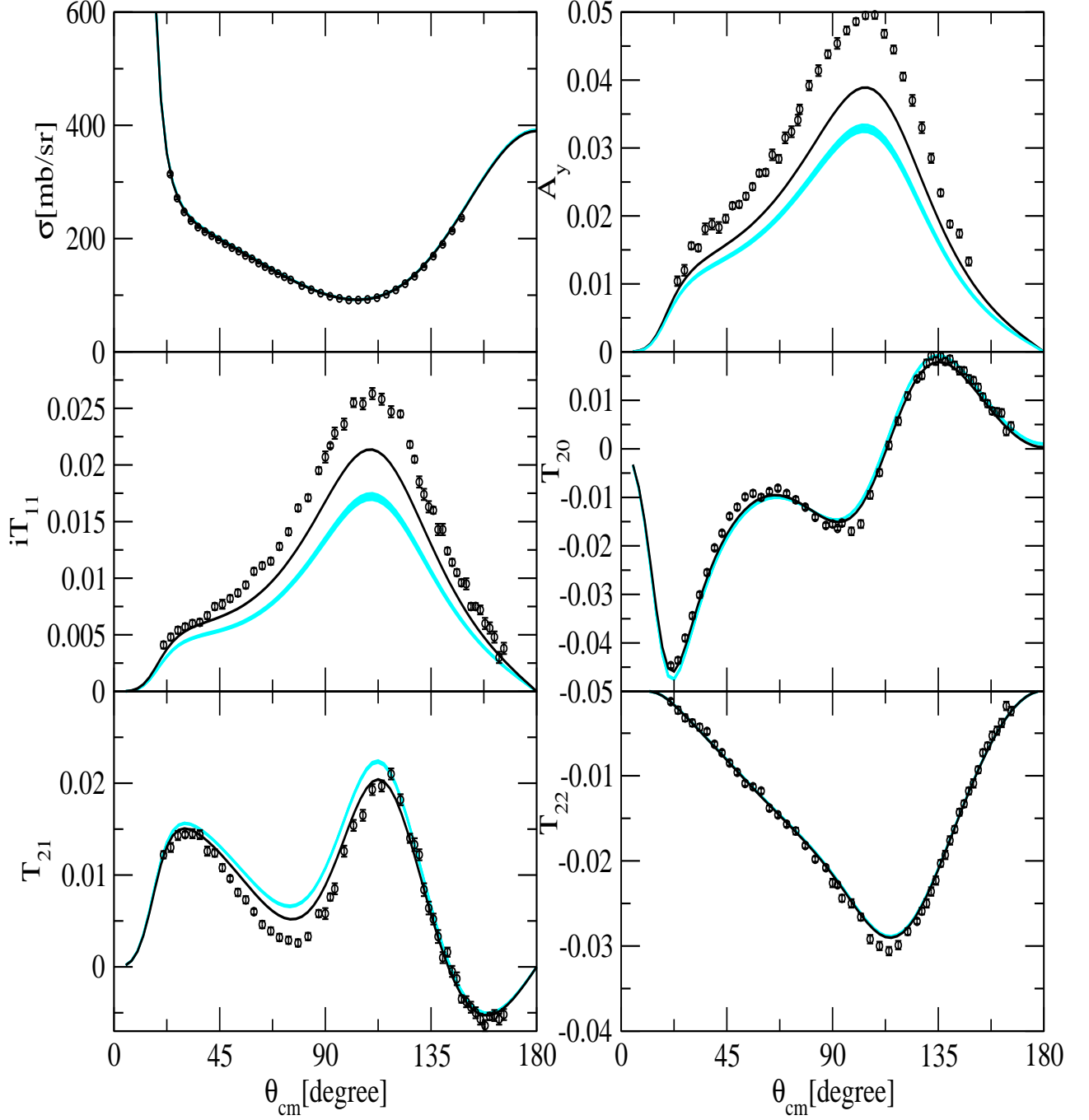


FIG. 8: (Color on line) Differential cross section and vector and tensor polarization observables at  $E_{lab} = 3$  MeV using the AV18+URIX model with the parameters given in Table III (cyan band). The predictions of the original AV18+URIX model, given in the first row of the table, are shown as a solid line. The experimental points from Ref. [25] are also shown.

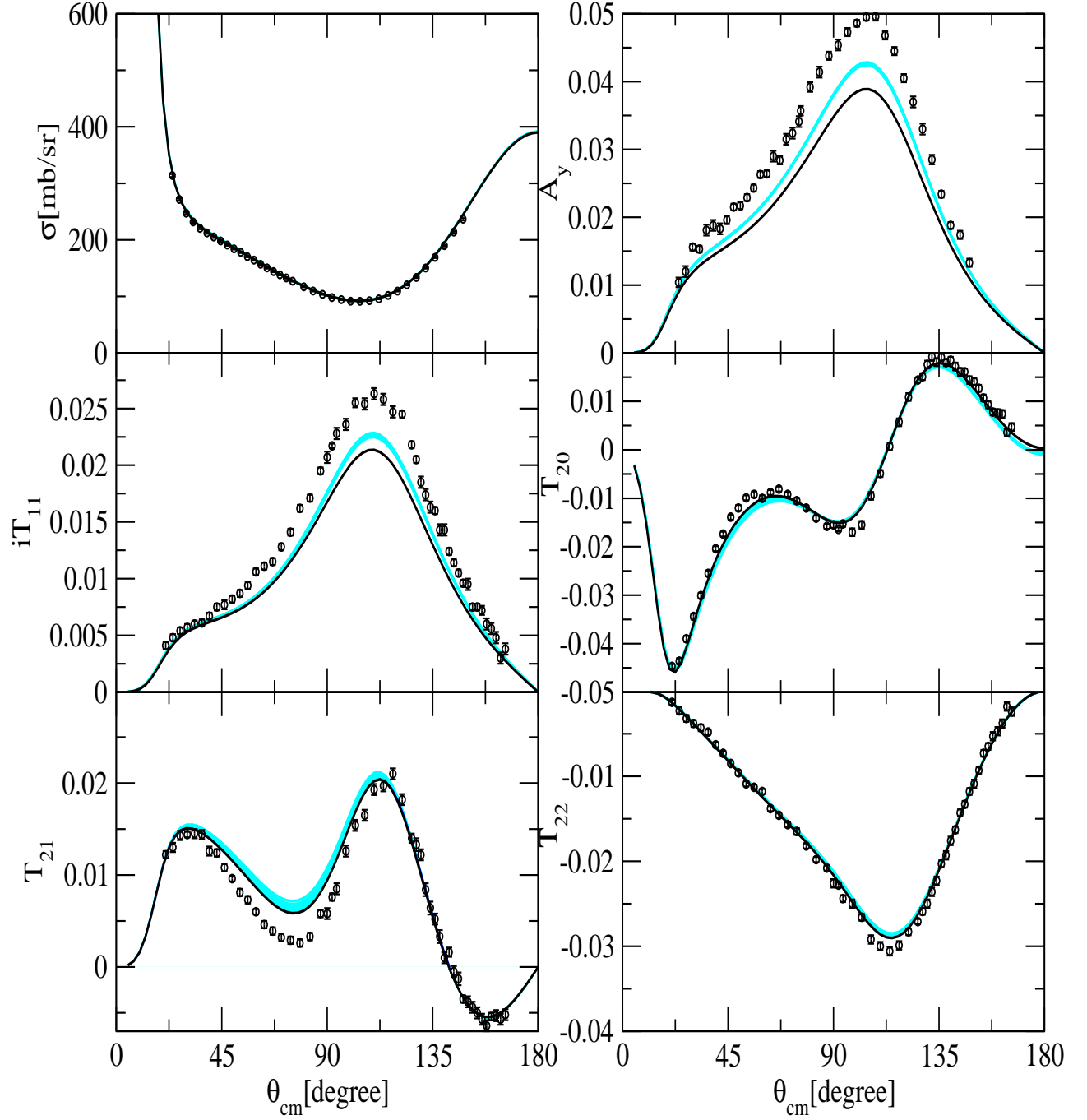


FIG. 9: (Color on line) Differential cross section and vector and tensor polarization observables at  $E_{\text{lab}} = 3$  MeV using the AV18+N2LOL model with the parameters given in Table IV (cyan band). The predictions of the AV18+URIX model (solid line) and the experimental points from Ref. [25] are also shown.

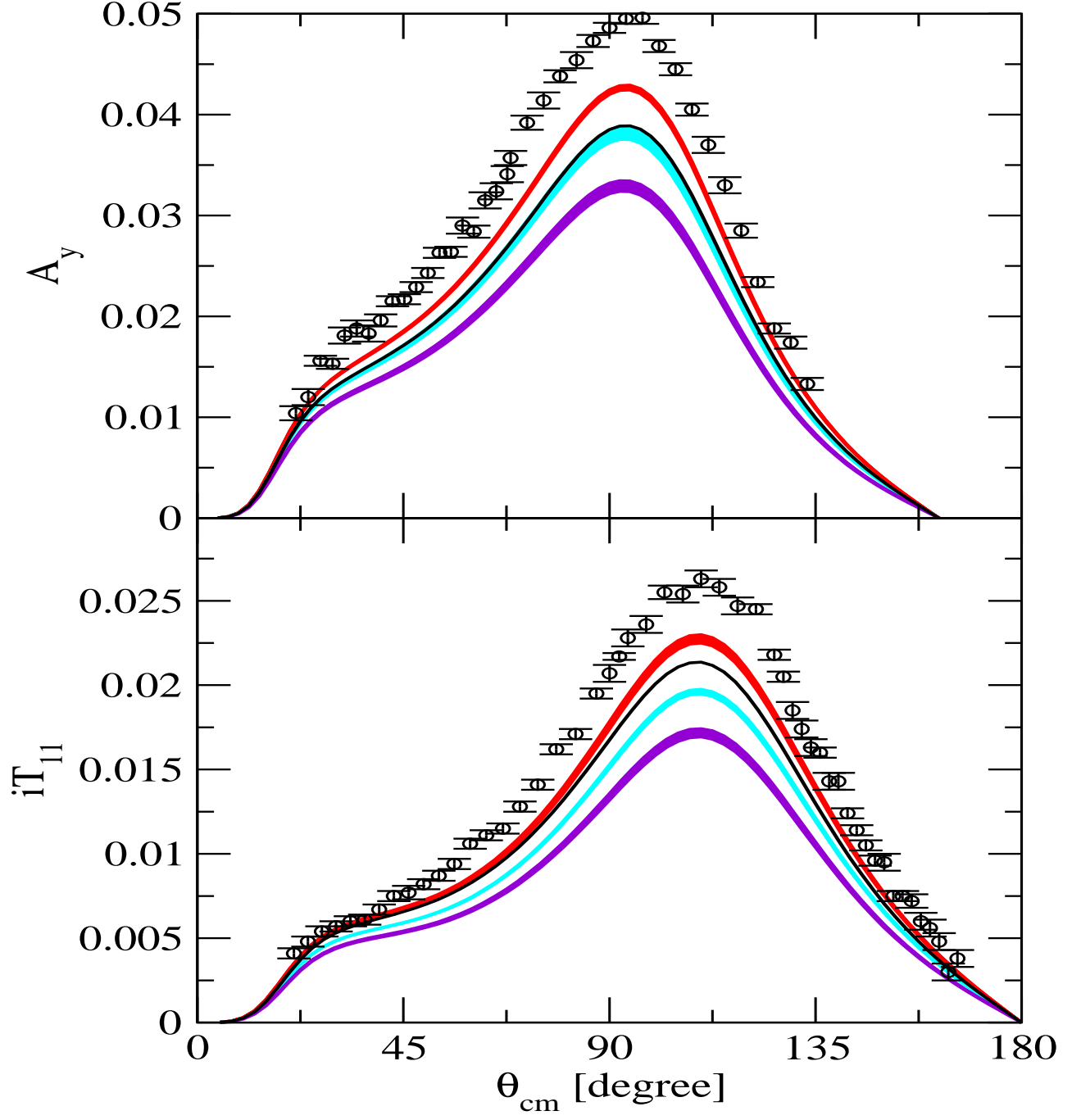


FIG. 10: (Color on line) The vector analyzing powers  $A_y$  and  $iT_{11}$  at  $E_{\text{lab}} = 3$  MeV using the AV18+TM' (cyan band), AV18+URIX (violet band) and AV18+N2LOL (red band) models as in Figs. 7,8,9. The predictions of the AV18+URIX model (solid line) and the experimental points from Ref. [25] are also shown.